

1 Supplementary File

2

3 *Investigating the interactions of the cucumber mosaic virus 2b protein with*
4 *the viral 1a replicase component and the cellular RNA silencing factor*
5 **Argonaute 1**

6 **Sam Crawshaw¹, Alex M. Murphy¹, Pamela J. E. Rowling², Daniel Nietlispach³, Laura S.**
7 **Itzhaki² and John P. Carr^{1*}**

8

9 1. Department of Plant Sciences, University of Cambridge, Downing Street, Cambridge CB2
10 3EA, United Kingdom

11 2. Department of Pharmacology, University of Cambridge, Tennis Court Rd, Cambridge CB2
12 1PD, United Kingdom

13 3. Department of Biochemistry, University of Cambridge, Sanger Building, 80 Tennis Court
14 Rd, Cambridge CB2 1GA, United Kingdom

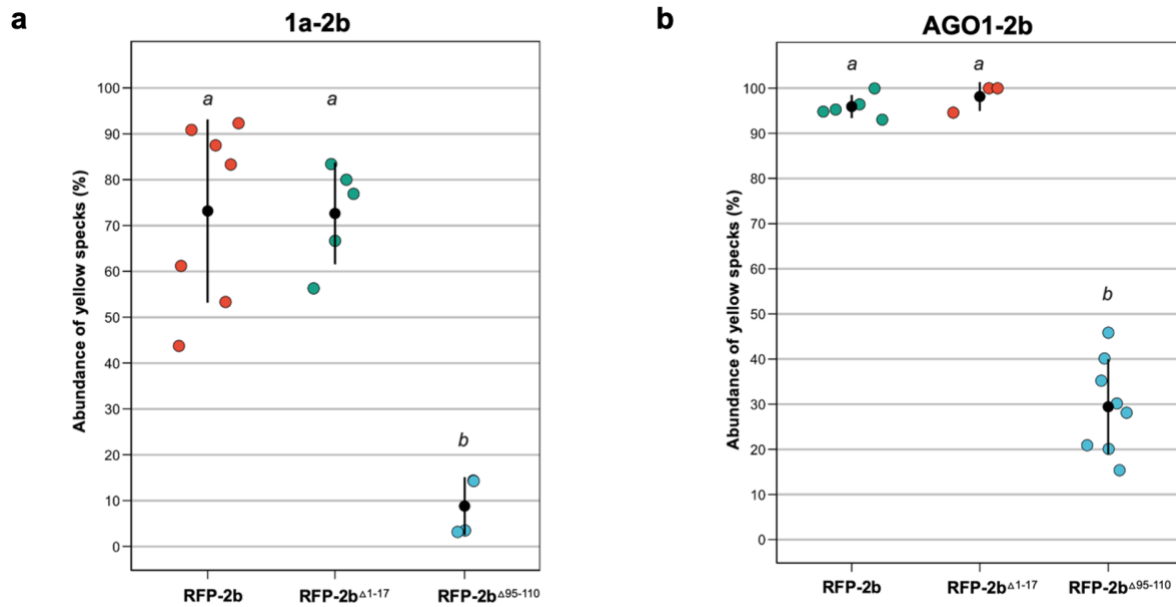
15 *Author for Correspondence: jpc1005@cam.ac.uk
16

17 **Table S1. Primer sequences.**

Primer name	Sequence (5'-3')
Gateway cloning	
2b attB Rv	GGGGACCACTTGTACAAGAAAGCTGGGTTGAAAGCACCTC CGCCCA
2b attB Fw	GGGGACAAGTTGTACAAAAAAGCAGGCTTCATGGAATTG AACGTAGGT
2bD1-17 Fw	GGGGACAAGTTGTACAAAAAAGCAGGCTTCATGGTGGA GGCGAAGAAC
2b Δ 95-110 Rv	GGGGACCACTTGTACAAGAAAGCTGGGTTAAAATCATG GTCTTCCGCCGA
2b Δ 85-110	GGGGACCACTTGTACAAGAAAGCTGGGTTACGAGAGGCCTC AGACTCG
2b Δ 74-110	GGGGACCACTTGTACAAGAAAGCTGGGTTACATGGCGGCA TGAC
2b Δ 56-110	GGGGACCACTTGTACAAGAAAGCTGGGTTAGGAAGCGGAA TAGTCTGAGATTGAAC
2b Δ 83-110 Rv	GGGGACCACTTGTACAAGAAAGCTGGGTTTCAGGCCTCAGA CTCGGG
2b Δ 1-55 Fw	GGGGACAAGTTGTACAAAAAAGCAGGCTTAATGCCGTTCTA TCAAGTGGATGGTCG
2b Δ 61-110 Rv	GGGGACCACTTGTACAAGAAAGCTGGGTTCACTGATAGAA CGGTAGGAAGCG
2b Δ 65-110 Rv	GGGGACCACTTGTACAAGAAAGCTGGGTTTCAGGCCTCAGC CACTTGATAGAACG
2b Δ 69-110 Rv	GGGGACCACTTGTACAAGAAAGCTGGGTTGACCCTGTCAG TTCCGAACC
Q5 mutagenesis	
2bLS/Fny83-93 Rv	GGCCTCAGACTCGGGTAA
2bLS/Fny83-93 Fw	TTTGACGATACAGATTGGTCG
2b Δ 56-60/65 Rv	TAGGAAGCGGAATAGTCTGAG
2b Δ 39-48 Fw	CTCAGACTATTCCGCTTCCTAC
2b Δ 39-48 Rv	GTGACCTCGTCCCGTCG
2b Δ 56-65 Fw	ACAGGGTCATGCCGC
2b Δ 56-60 Fw	GATGGTCGGAACTGACAG
2b56aaa65 Rv	CGCCGCCGCCGCCGCCGCCGCCGCTAGGAAGCGGAATAGTCTGAG TAGTCTGAG
2b56aaa60 Rv	CGCCGCCGCCGCCGCTAGGAAGCGGAATAGTCTGAG
2bFny/LS56-60 Fw	CCGTTCCatggAGTGGATGGTCGGAA
2b Δ 83-93 (step 2) Rv	GAAAGCACCTCCGCCATTGTTACCGGCGAACCAATCTGT ATCGTCAAAGGCCTC
2b Δ 83-93 (step 1) Rv	CCAATCTGTATCGTCAAAGGCCTCAGACTCGGGTAAC
2b Fw	ATGGAATTGAACGTAGGTGCAATGAC

18

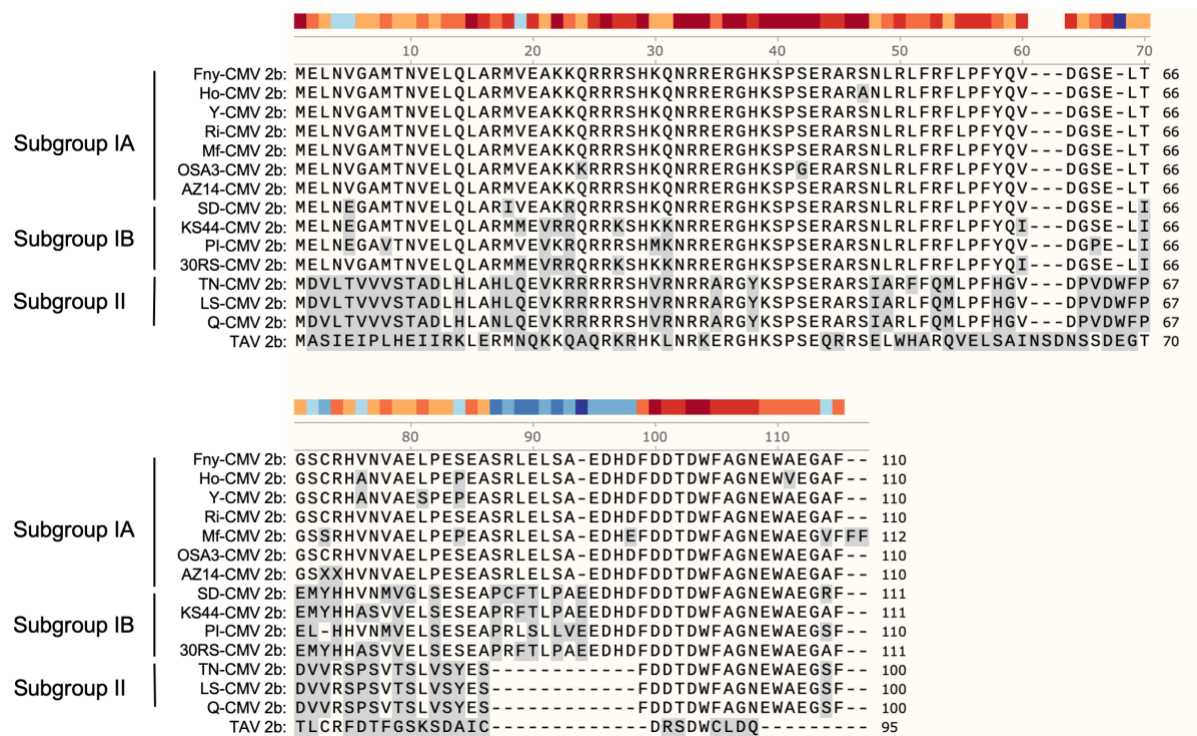
19



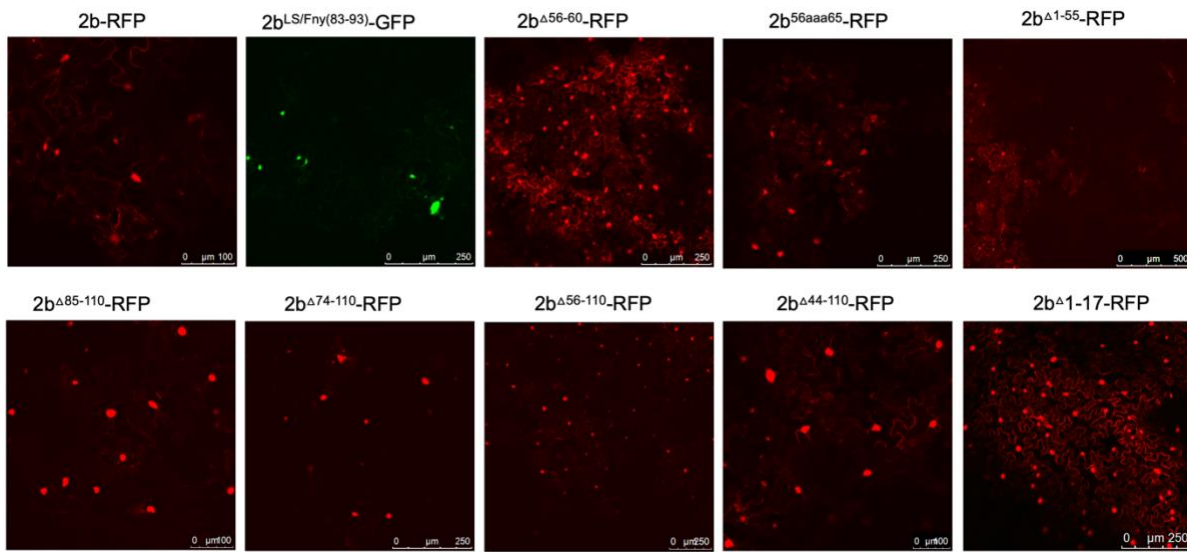
20

Fig. S1 The C-terminal domain of the cucumber mosaic virus 2b protein enhances its interaction with the Fny-CMV 1a and AGO1 proteins. Red fluorescent protein (RFP)-tagged CMV 2b proteins containing deletions in their N-terminal domain ($\text{RFP-2b}^{\Delta 1-17}$) or C-terminal domain ($\text{RFP-2b}^{\Delta 95-110}$) were transiently co-expressed with green fluorescent protein (GFP)-tagged Fny-CMV 1a or AGO1 proteins in agroinfiltrated leaves of *N. benthamiana*. The abundance of yellow specks in each image was quantified by calculating the number of yellow specks as a percentage of the total specks present in the image. Individual abundance values are presented as jitter plots with each mean value and standard error depicted as black bars. Since yellow specks result from the overlay of GFP and RFP fluorescent signals they were used as a measure of co-localisation between co-infiltrated GFP- and RFP-tagged proteins. **a** Co-localisation results for 1a-GFP with $\text{RFP-2b}^{\Delta 95-110}$, $\text{RFP-2b}^{\Delta 1-17}$ and RFP-2b. Lower case letters *a* and *b* indicate mean values for abundance of yellow specks that are significantly different from each other ($P < 0.0001$: Tukey's multiple comparison of means). Values labelled with the same letter are not significantly different from each other. Deletion of the N-terminal domain of the 2b protein had no significant effect on colocalisation with CMV 1a proteins. However, deletion of the C-terminal domain of the 2b protein significantly reduced colocalisation with CMV 1a proteins. **b** Co-localisation results for AGO1-GFP with $\text{RFP-2b}^{\Delta 95-110}$, $\text{RFP-2b}^{\Delta 1-17}$ and RFP-2b. Lower case letters *a* and *b* indicate mean values for abundance of yellow specks that are significantly different from each other ($P < 0.0001$: Tukey's multiple comparison of means). Values labelled with the same letter are not significantly different from each other. Deletion of the N-terminal domain of 2b had no significant effect on colocalisation with AGO1 proteins. However, deletion of the C-terminal domain of 2b significantly reduced colocalisation with AGO1 proteins. Number of independent leaves imaged for each treatment, $n \geq 3$.

45



47 **Fig. S2** The amino acid sequences of 2b proteins encoded by a selection of strains of *Cucumber*
 48 *mosaic virus* (CMV) from Subgroups IA, IB and II and the 2b protein from *Tomato aspermy*
 49 virus (TAV). The Fny-CMV 2b protein sequence is given as a reference to compare with 2b
 50 protein sequences from a small number of other CMV strains to highlight certain differences
 51 and similarities between 2b proteins of viruses in Subgroups IA, IB and II. Differences in 2b
 52 protein primary sequences between the Fny-CMV and other strains are highlighted in grey.
 53 The numbering of amino acid residues is based on the Fny-CMV 2b protein sequence. The
 54 GenBank accession numbers for the sequences used in this alignment are NC002035 for Fny-
 55 CMV (2b-Fny), D12538 for Y-CMV (2b-Y), LC593245 for Ho- CMV (2b- Ho), AM183118
 56 for RI-8-CMV (2b-RI-8), AJ276480 for Mf-CMV (2b-Mf), HE971489 for OSA3-CMV (2b-
 57 OSA3), QBH72281 for AZ14-CMV (2b-AZ14), D86330 for SD-CMV, CBG76802 for KS44-
 58 CMV (2b-KS44), CAJ65577 for PI-1-CMV (2b-PI-1), FN552601 for 30RS-CMV (2b-30RS),
 59 BAD15371 for TN-CMV (2b-TN), AF416900 for LS-CMV (2b- LS), Q66125 for Q-CMV
 60 (2b-Q) and AJ320274 for KC-TAV (TAV 2b).



62

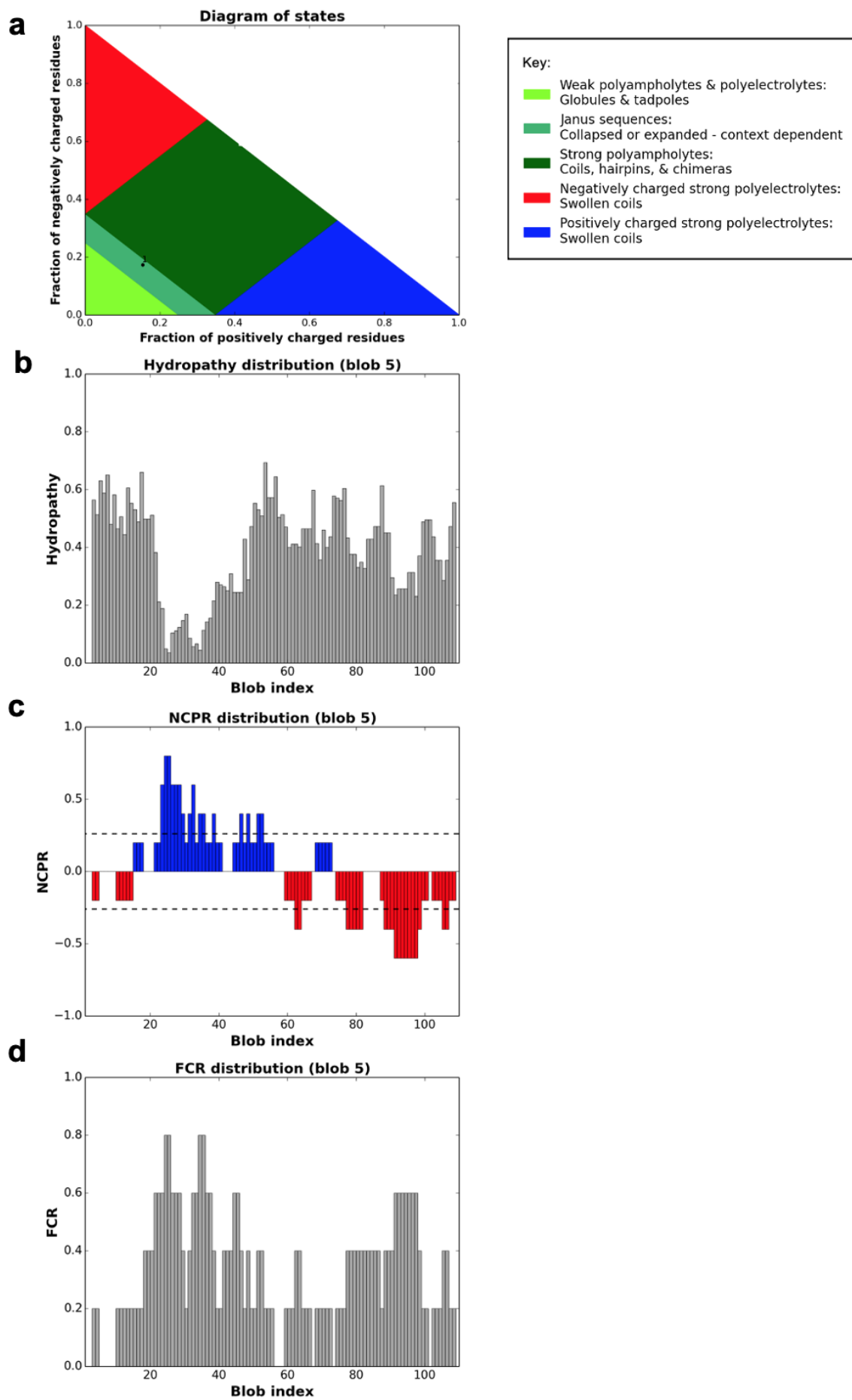
63

Fig. S3 Mutations affecting the subcellular localization of cucumber mosaic virus 2b proteins. Agroinfiltration was used for transient expression in *N. benthamiana* leaves of C-terminal red fluorescent protein 2b-(RFP) or C-terminal green fluorescent protein 2b-(GFP) fusion protein. All mutant versions of the 2b protein showed nuclear and cytoplasmic localisation. However, mutant versions of the 2b protein lacking residues at their C-terminus (such as 85-110, 74-110, 56-110 or 44-110) showed an increased nuclear localisation compared to the wild-type protein. Increased nuclear localisation was also seen for the LS/Fny chimeric mutant in which residues present in the Fny-CMV 2b protein (residues 83-93) but absent in the sequence of the LS-CMV 2b protein, were introduced into a chimeric LS-CMV protein. However, the N-terminal mutant from residues 1-17, mutations from 56-60 or substitution of alanine from 56-60 had no impact on the localisation of CMV 2b. In contrast, deletion of residues from 1-55 caused a reduction in nuclear localisation and an increase in cytoplasmic localisation.

76

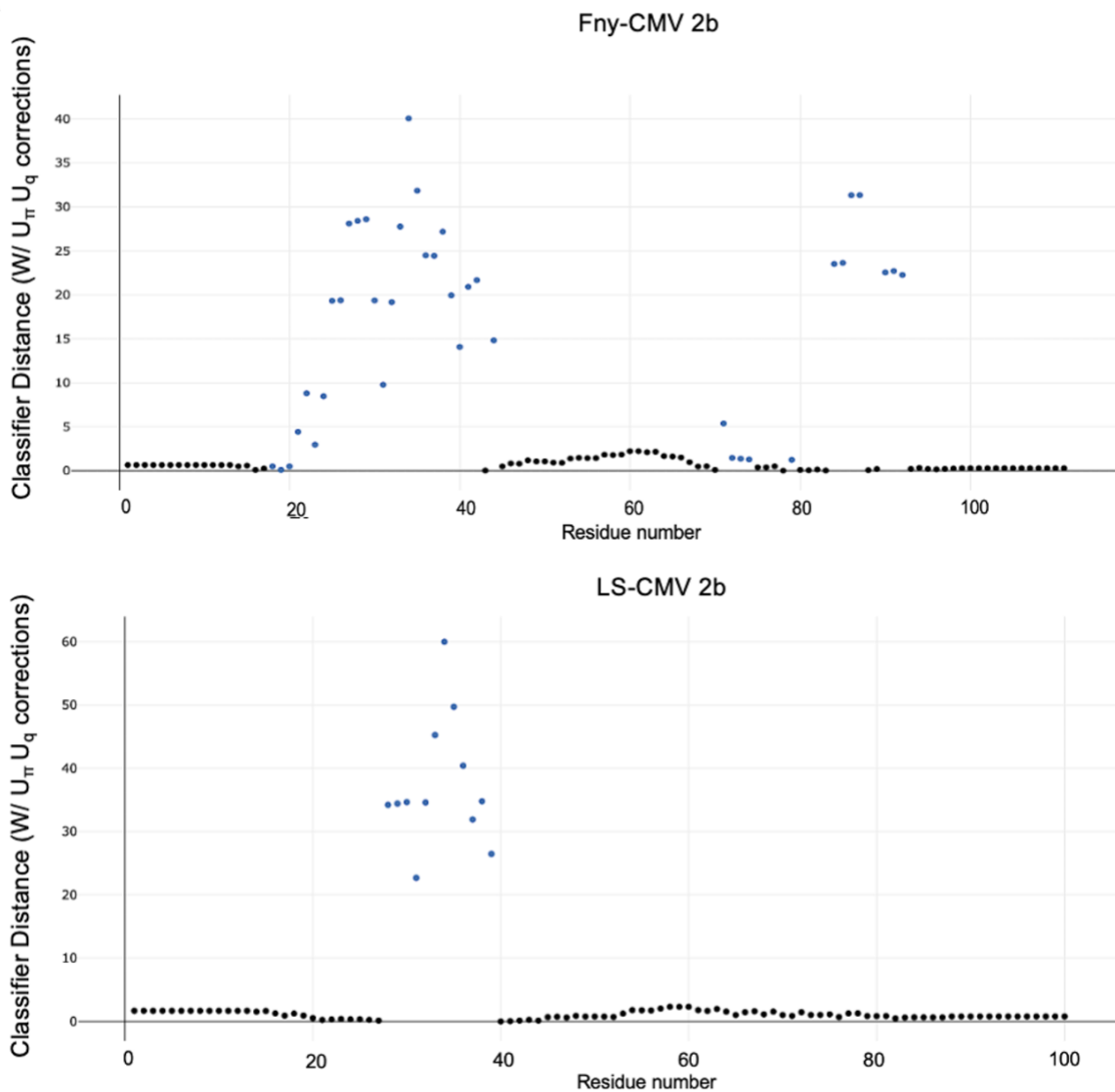
77

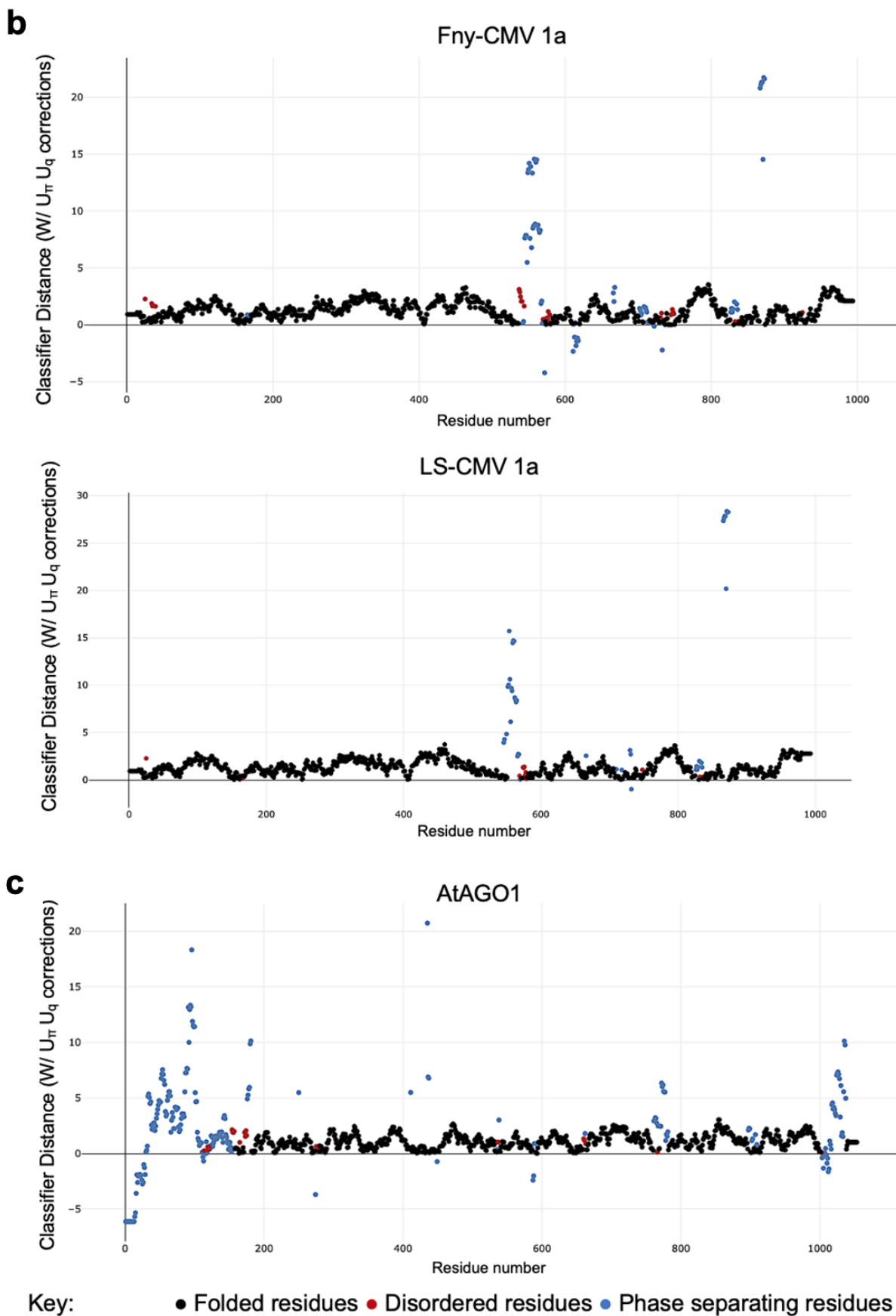
78



80 **Fig. S4** Prediction of physicochemical properties for the Fny-CMV 2b protein. This figure
81 shows the predictions of the CIDER server (<http://pappulab.wustl.edu/CIDER/about/>). **a** The
82 diagram of states provides an estimate of the kinds of ensembles adopted by an intrinsically
83 disordered sequence. The predictions suggest that the Fny-CMV 2b protein sequence has a
84 context-dependent structure, existing in either collapsed or expanded states depending on other
85 factors such as salt concentration, ligand binding, *cis*- interactions etc. **b** The mean hydrophathy
86 of the sequence shown as a re-scaled Kyte-Doolittle (Kyte and Doolittle, 1982) hydrophathy
87 value which lies between 0 (least hydrophobic) and 1 (most hydrophobic). **c** The net charge
88 per residue (NCPR) predicts that the Fny- CMV 2b protein has clearly grouped regions of
89 positive and negative charge. **d** The fraction of charged residues in the sequence (FCR) also
90 shows grouping of regions with charged residues. This may facilitate self-interaction and the
91 regions of positive charge are likely candidates for RNA interaction.

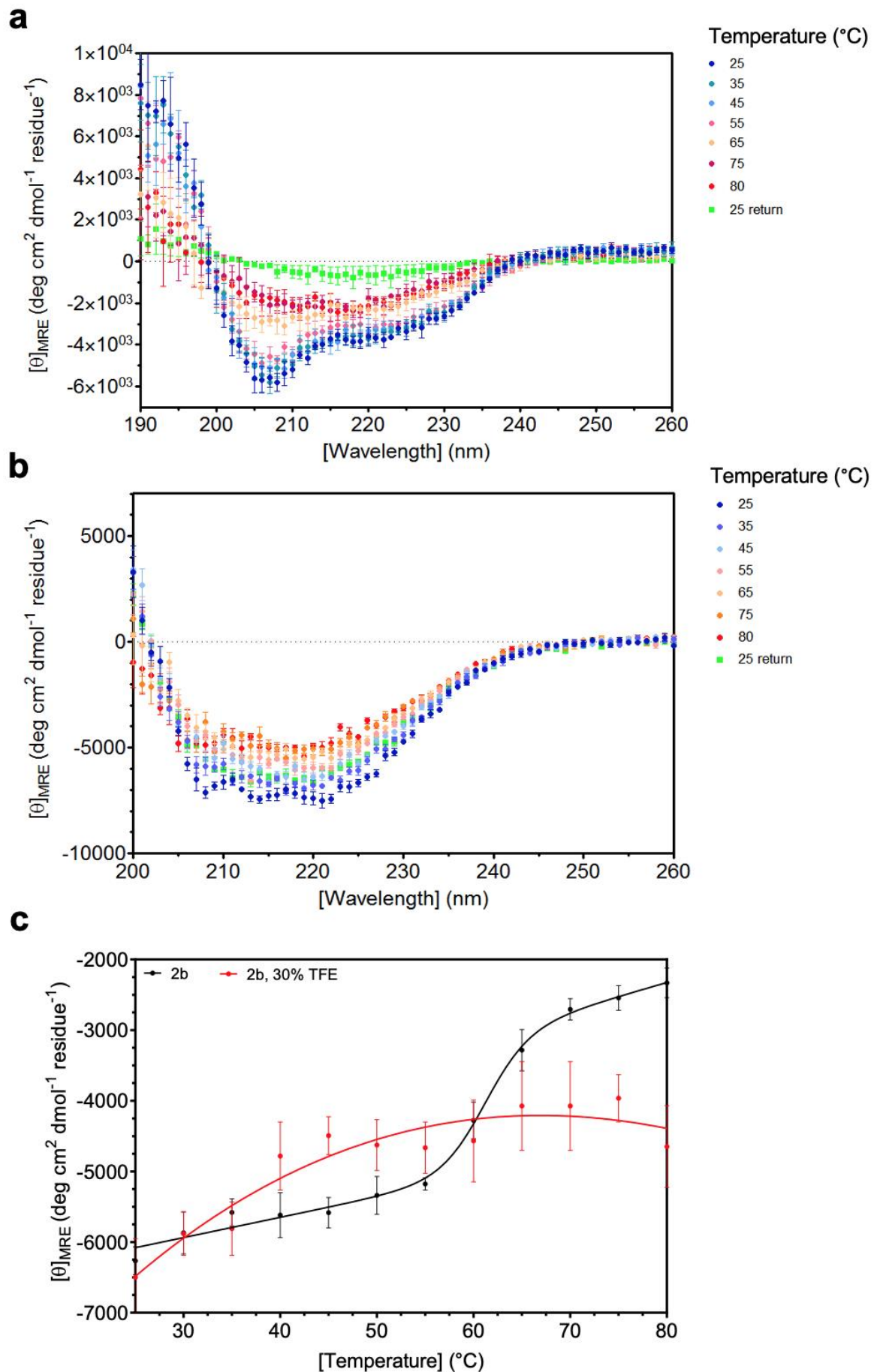
92

a



96 **Fig. S5** Predictions of phase separation. The ParSe v2 program identifies protein regions likely
97 to exhibit physiological phase separation behaviour. The results shown here are for the
98 modified ParSe v2 program accounting for the effects of interactions between amino acids
99 (termed U_{π} for $\pi-\pi$ and cation- π interactions and U_q for charge-based effects). Residues are
100 colour coded based on their predicted state with black representing folded residues, red
101 representing disordered residues and blue representing phase separating residues. The classifier
102 distance on the Y-axis represents the confidence in the assigned states with higher values
103 relating to higher confidence. **a** The Fny-CMV 2b protein is predicted to contain two regions
104 which are promote phase separation behaviour while the LS-CMV 2b protein contains only
105 one such region. **b** The Fny-CMV 1a protein contains residues which are likely to promote
106 phase separating behaviour, but these represent a smaller percentage of residues than those
107 seen in the Fny-CMV 2b protein. The LS-CMV 1a protein also contains residues which are
108 likely to promote phase separation, but there are slightly fewer such residues than in the Fny-
109 CMV 1a protein (41 compared with 66). **C**, The *A. thaliana* AGO1 protein is also predicted to
110 contain residues promoting phase separation with the greatest density at its N-terminus.

111

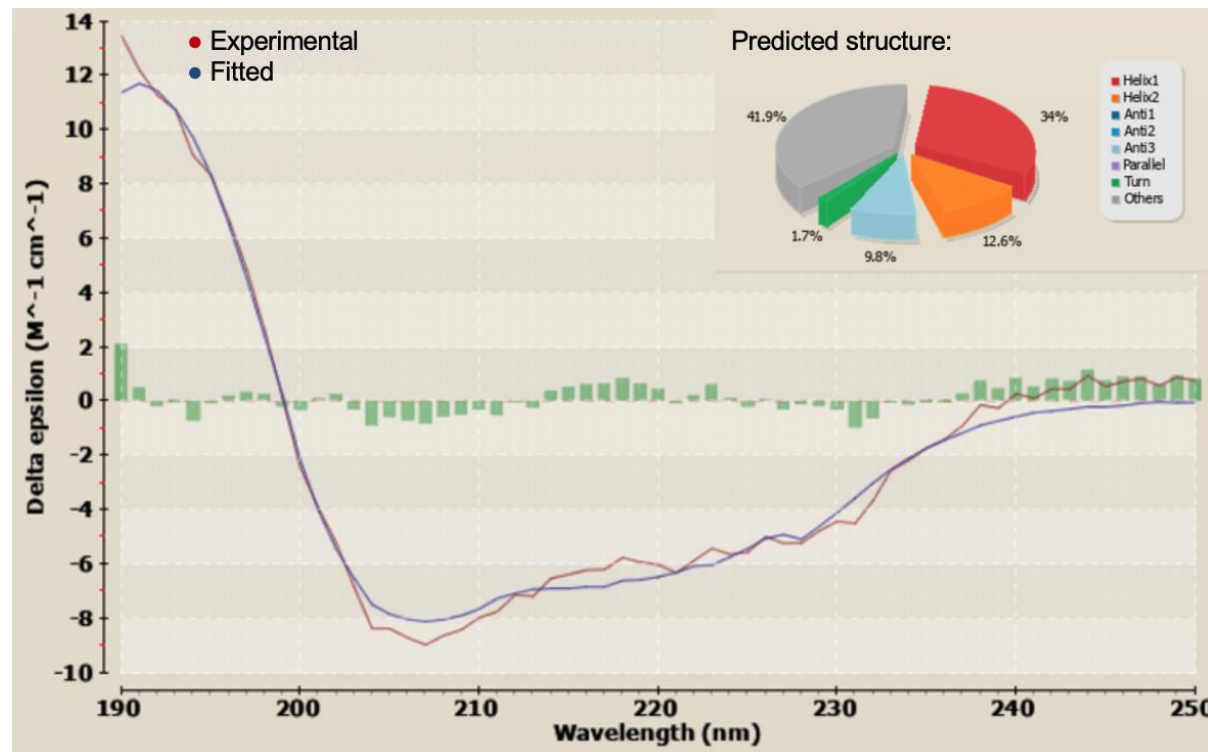


113
114 **Fig. S6** Temperature Denaturation of the Fny-CMV 2b protein. Circular dichroism data were
115 obtained at a protein concentration of 13.5 μ M 2b in 10 mM Phosphate buffer pH 7.5 at
116 temperatures ranging from 25 °C to 80 °C. **a** Following heating, the 2b protein is irreversibly
117 denatured as cooling (green symbols) does not revert the protein to its initial state at 25 °C
118 (dark blue symbols). **b** Following the addition of 30% trifluroethanol (alpha-helical structure
119 in proteins) the 2b protein does not completely unfold even when heated to 80 °C and following
120 cooling back to 25 °C the protein does revert back to its initial folded state. **c** There is a
121 transition between folded and unfolded state where 50% of the 2b protein is in each state at 61
122 °C when fitted to a Boltzmann model with sloping baselines (black symbols) measured at 208
123 nm. All results are shown as the mean of five scans \pm SEM.

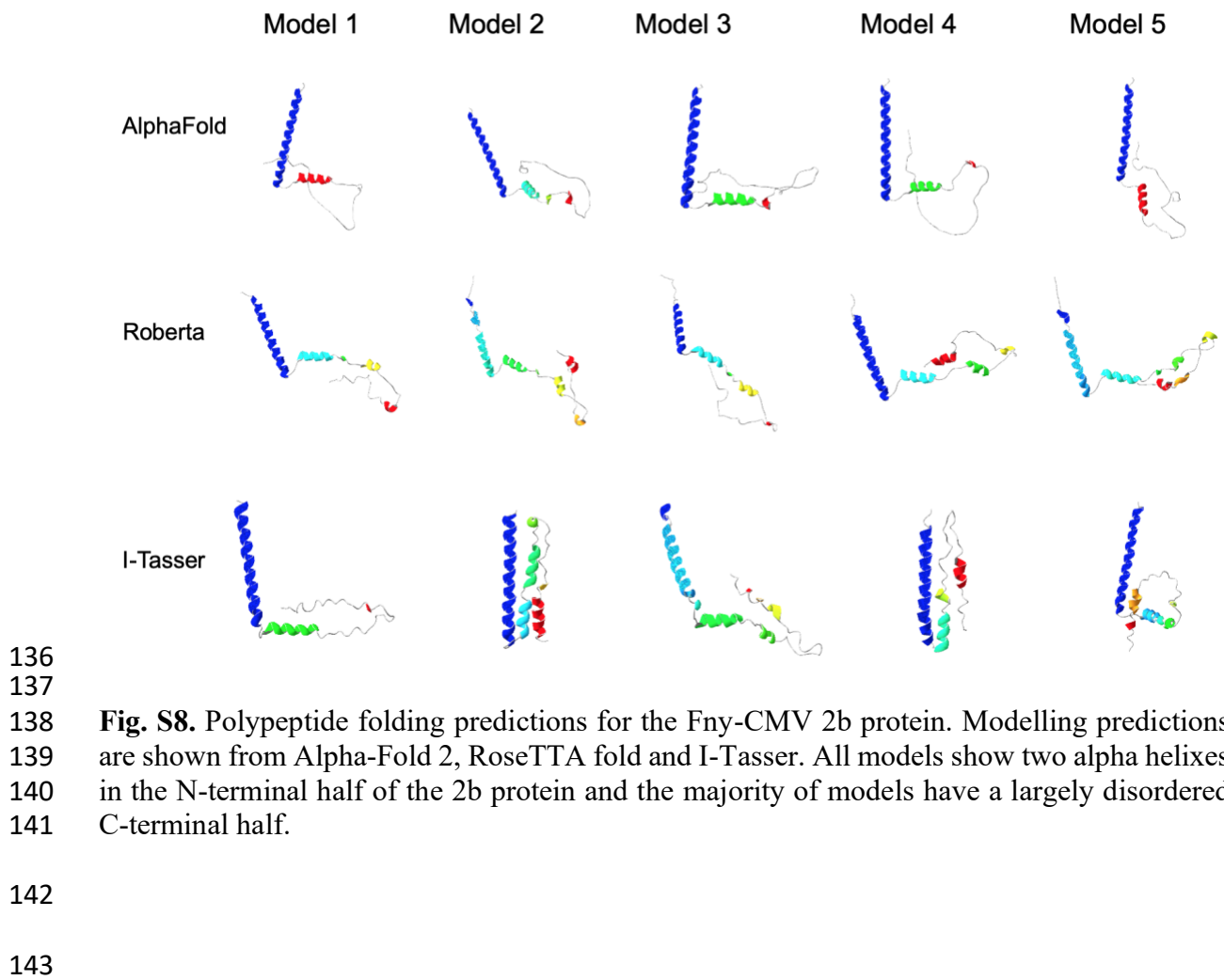
124

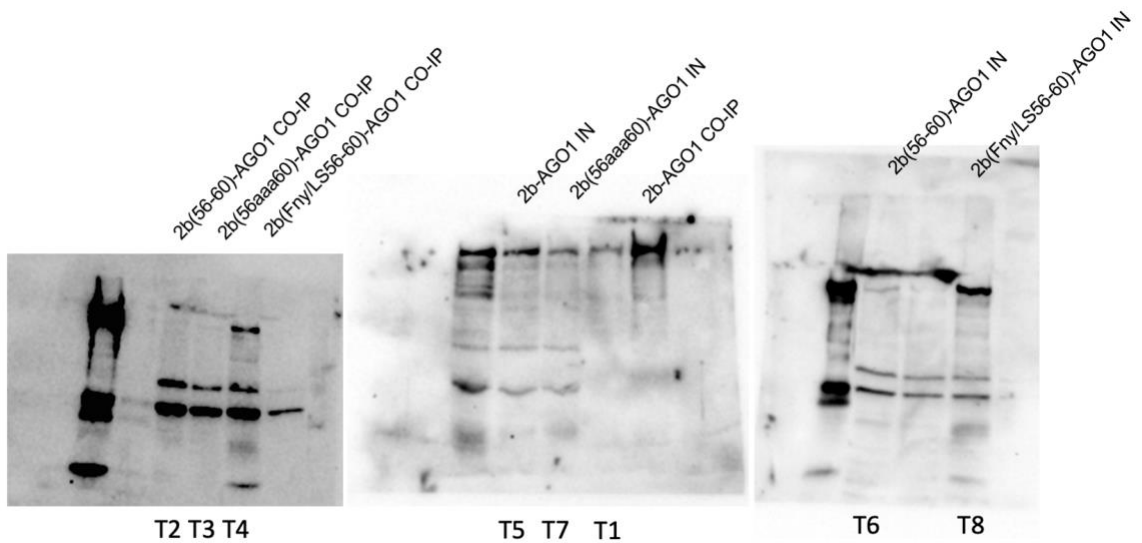
125

126



127
128
129 Fig. S7 Alternate analysis of circular dichroism data. The circular dichroism data shown in fig
130 9 for Fny-CMV 2b protein in the absence of TFE was also run through the BeStSel program
131 (v1.3.230210). This program predicted a similar level of disorder within the 2b sequence (41.9
132 %) but a larger percentage of alpha helical residues (46.6 %) and a smaller percentage of beta
133 sheet (9.8 %). This program does not use datasets specifically trained on disordered sequences
134 but the results do align more closely with the structural data obtained from NMR analysis.
135

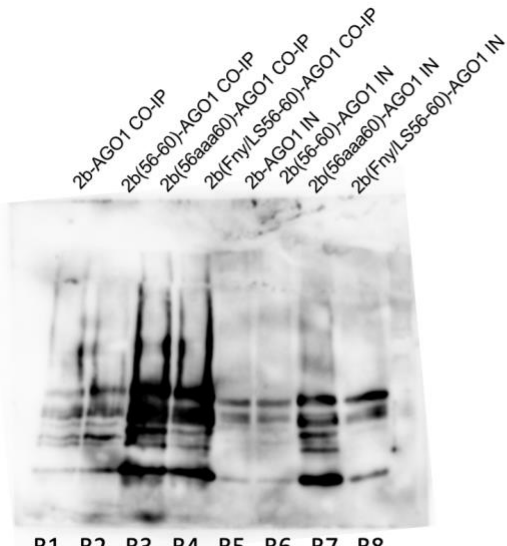


a

T2 T3 T4

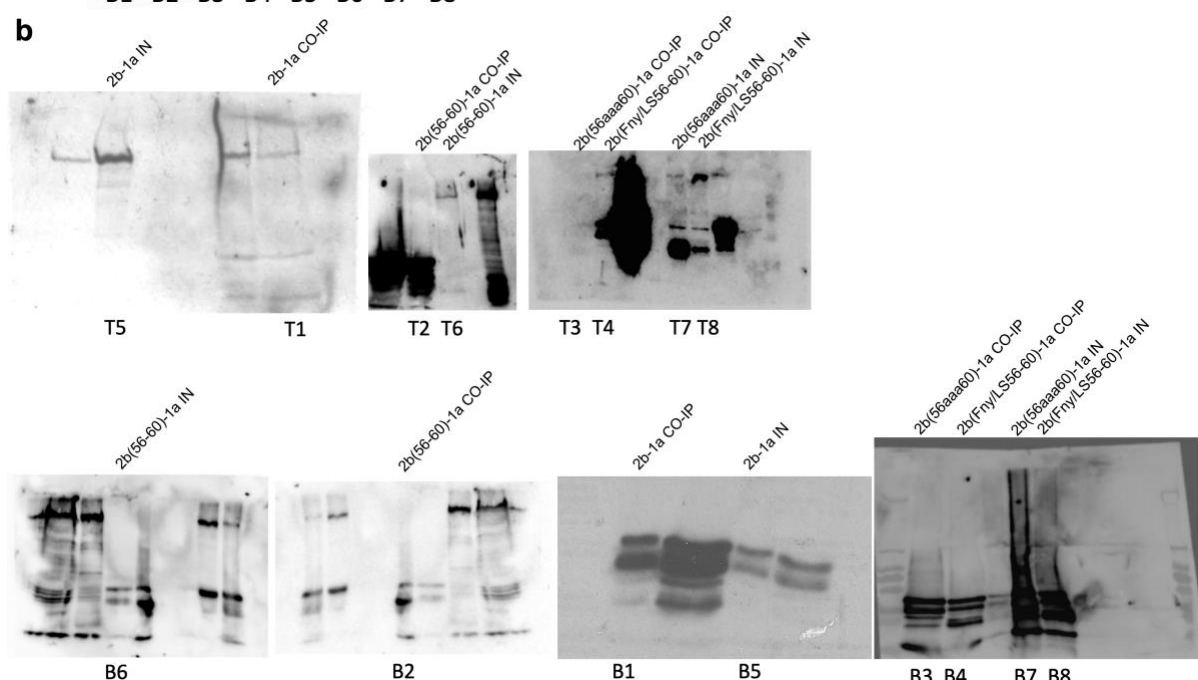
T5 T7 T1

T6 T8



B1 B2 B3 B4 B5 B6 B7 B8

144

b

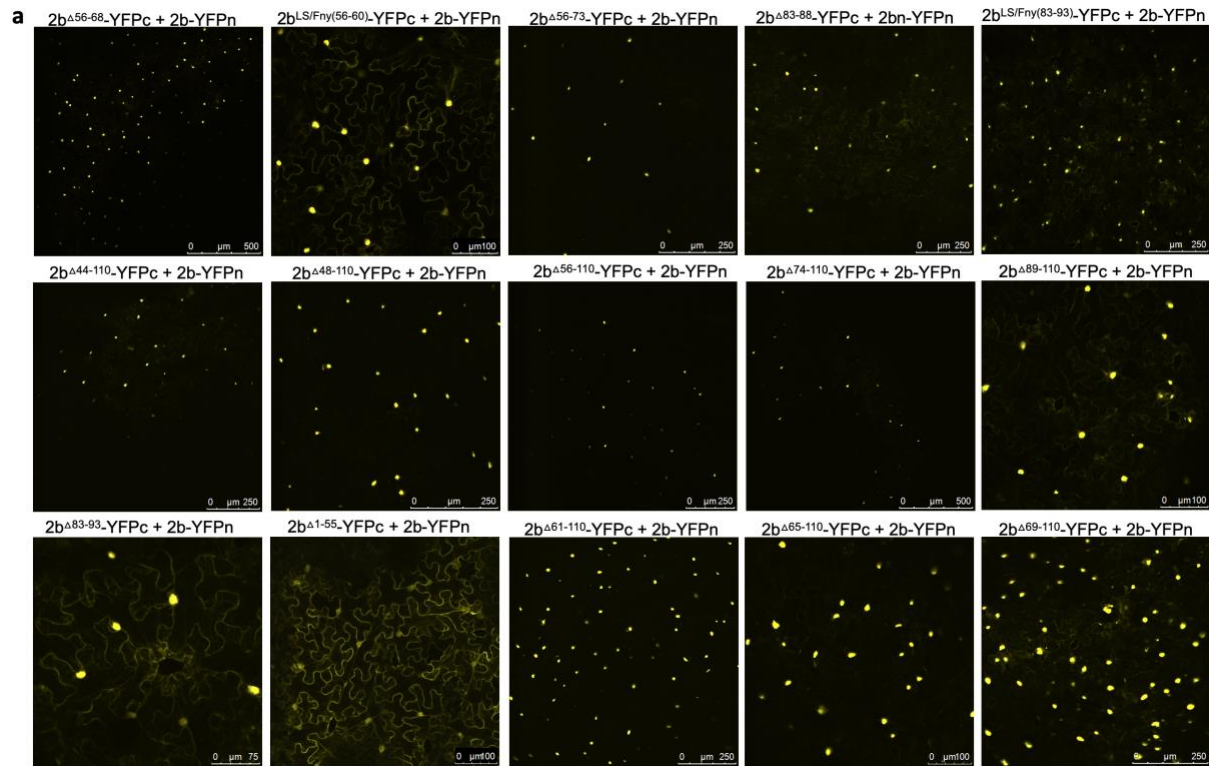
145

146 **Fig. S9** Whole gel images showing association of wild type and mutant Fny-CMV 2b proteins
147 with Fny-CMV 1a or AGO1 proteins demonstrated by co-immunoprecipitation. **a.** RFP- tagged
148 2b proteins were co-expressed with GFP tagged AGO1 proteins in *N. benthamiana* leaves.
149 Total protein was subjected to immunoprecipitation with GFP-Trap or RFP-Trap beads
150 followed by immunoblot analysis with anti-RFP antibodies to detect 2b- RFP or anti-GFP
151 antibodies to detect GFP-AGO1. Bands are labelled with the contents of the total protein
152 extract and treatment: input sample (IN), Co-immunoprecipitation with interacting partner
153 (CO-IP). The position where each band appears in the composite blot figures is denoted by T
154 or B referring to the top or bottom row of gel strips. **b.** RFP- tagged 2b proteins were co-
155 expressed with GFP tagged 1a proteins in *N. benthamiana* leaves. Total protein was subjected
156 to immunoprecipitation with GFP-Trap or RFP-Trap beads followed by immunoblot analysis
157 with anti-RFP antibodies to detect 2b-RFP or anti-GFP antibodies to detect GFP-1a. Bands are
158 labelled with the contents of the total protein extract and treatment: input sample (IN) or Co-
159 immunoprecipitation with interacting partner (CO-IP). The position where each band appears
160 in the composite blot figures is denoted by T or B referring to the top or bottom row of gel
161 strips.

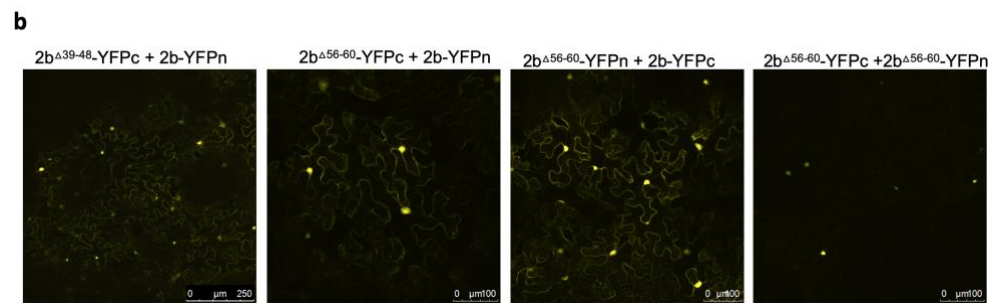
162

163

164



165



166

167 **Fig. S10** Mutations affecting the ability of 2b protein to interact with other CMV 2b proteins.
168 Bimolecular fluorescence complementation was used to compare the self-interaction properties
169 of the 2b proteins of Fny-CMV with mutant versions of the 2b protein using fusion proteins
170 with the N- and C-terminal domains of the yellow fluorescent protein (2b-YFPn and 2b-YFPc).
171 **a.** All mutant proteins were able to form heterodimers with WT 2b proteins *in vivo*, indicated
172 by yellow fluorescence. The intracellular distributions of these homodimers were consistent
173 with those seen for 2b-RFP or 2b-GFP mutant proteins and show a greater proportion of some
174 mutant 2b proteins being present in the nucleus. **b.** Tagged mutant versions of the 2b protein
175 lacking residues between 56-60 interacted strongly with tagged full length 2b proteins.
176 However, self-interaction with two mutant versions of the 2b protein resulted in markedly
177 reduced levels of self-interaction.

178

179

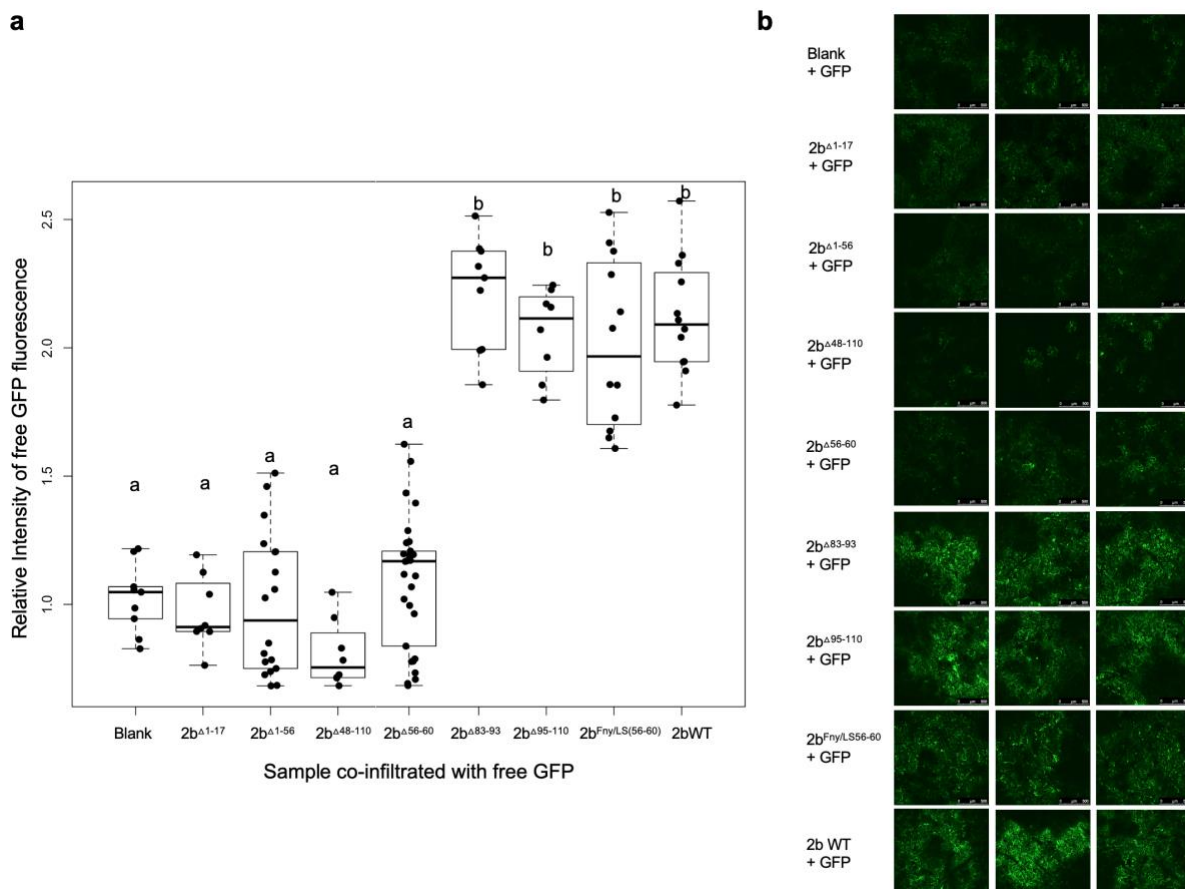
180
181182
183
184
185
186
187
188
189
190
191
192
193
194
195
196
197
198
199

Fig. S11 Mutations in the C-terminal region of the CMV 2b protein do not impact its RNA silencing suppressor activity. Green fluorescent protein (GFP) was expressed transiently, under a 35S promoter, in agroinfiltrated leaves of *Nicotiana benthamiana*. **a.** The relative intensity of GFP fluorescence was quantified using ImageJ as the integrated density (IntDen) of each image, for each treatment 12 days after infiltration. Individual relative fluorescence values are presented as jitter plots with each mean value and standard error depicted as black bars. Compared to the intensity of fluorescence emitted by leaves expressing GFP only, the relative intensity values of GFP fluorescence emitted by leaf tissue agroinfiltrated with mixtures of *A. tumefaciens* cells that included those carrying constructs expressing the full length 2b protein (WT), 95-110, 83-93 or Fny/LS(56-60) mutant versions of the 2b protein were significantly greater. Lower case letters *a* and *b* indicate mean values for relative fluorescence intensity that are significantly different from each ($P < 0.0001$: Tukey's multiple comparison of means). Values labelled with the same letter are not significantly different from each other. Number of independent leaves imaged for each treatment, $n > 6$. **b.** Typical confocal images of GFP fluorescence in the presence of full length or mutant versions of the CMV 2b protein as indicated.